

See discussions, stats, and author profiles for this publication at: <https://www.researchgate.net/publication/51663155>

Low temperature FTIR spectroscopy provides new insights in the pH-dependent proton pathway of proteorhodopsin

ARTICLE *in* BIOCHIMICA ET BIOPHYSICA ACTA · SEPTEMBER 2011

Impact Factor: 4.66 · DOI: 10.1016/j.bbabo.2011.09.001 · Source: PubMed

CITATIONS

7

READS

23

7 AUTHORS, INCLUDING:



Sarika Shastri

Goethe-Universität Frankfurt am Main

8 PUBLICATIONS 190 CITATIONS

SEE PROFILE



Clemens Glaubitz

Goethe-Universität Frankfurt am Main

124 PUBLICATIONS 2,154 CITATIONS

SEE PROFILE



Werner Mänteke

Goethe-Universität Frankfurt am Main

85 PUBLICATIONS 1,347 CITATIONS

SEE PROFILE



Josef Wachtveitl

Goethe-Universität Frankfurt am Main

180 PUBLICATIONS 3,740 CITATIONS

SEE PROFILE



Low temperature FTIR spectroscopy provides new insights in the pH-dependent proton pathway of proteorhodopsin

Mirka-Kristin Verhoeven^{a,1}, Gabriela Schäfer^{b,1}, Sarika Shastri^c, Ingrid Weber^c, Clemens Glaubitz^c, Werner Mäntele^{b,*}, Josef Wachtveitl^{a,**}

^a Institute of Physical and Theoretical Chemistry, Johann Wolfgang Goethe-University Frankfurt, Max-von-Laue Straße 7, 60438 Frankfurt am Main, Germany

^b Institute of Biophysics, Johann Wolfgang Goethe-University Frankfurt, Max-von-Laue Straße 1, 60438 Frankfurt am Main, Germany

^c Institute of Biophysical Chemistry, Johann Wolfgang Goethe-University Frankfurt, Max-von-Laue Straße 9, 60438 Frankfurt am Main, Germany

ARTICLE INFO

Article history:

Received 8 June 2011

Received in revised form 25 August 2011

Accepted 5 September 2011

Available online 11 September 2011

Keywords:

Proteorhodopsin

Photocycle

pH dependence

FTIR spectroscopy

Low temperature

ABSTRACT

In the presented study the low pH photocycle of proteorhodopsin is extensively investigated by means of low temperature FTIR spectroscopy. Besides the already well-known characteristics of the all-*trans* and 13-*cis* retinal vibrations the 77 K difference spectrum at pH 5.1 shows an additional negative signal at 1744 cm⁻¹ which is interpreted as indicator for the L state. The subsequent photocycle steps are investigated at temperatures higher than 200 K. The combination of visible and FTIR spectroscopy enabled us to observe that the deprotonation of the Schiff base is linked to the protonation of an Asp or Glu side chain – the new proton acceptor under acidic conditions. The difference spectra of the late intermediates are characterized by large amide I changes and two further bands ((-1751 cm⁻¹)/(+1725 cm⁻¹) in the spectral region of the Asp/Glu $\nu(\text{C}=\text{O})$ vibrations. The band position of the negative signature points to a transient deprotonation of Asp-97. In addition, the pH dependence of the acidic photocycle was investigated. The difference spectra at pH 5.5 show distinct differences connected to changes in the protonation state of key residues. Based on our data we propose a three-state model that explains the complex pH dependence of PR.

© 2011 Elsevier B.V. All rights reserved.

1. Introduction

During the last decade proteorhodopsins (PR) have been discovered in uncultivated marine proteobacteria in various oceanic ecosystems [1–6]. They were found to be light-driven proton pumps and can be mainly classified in two families [1,7]: Green-absorbing PR (GPR) and blue-absorbing PR (BPR). Interestingly, GPRs can be converted to BPRs (and vice versa) by a single point mutation [3]. Apart from their absorption maximum, GPRs and BPRs also differ in their photochemical properties. GPRs show a faster photocycle rate and exhibit a remarkably higher proton pumping activity. BPRs are therefore discussed to play a more regulatory rather than an energy converting role [3]. The wide distribution in different environments and the different functions show that PRs are most likely a key determinant for the phototrophic energy balance of the biosphere.

Structural information about this class of proteins is therefore crucial to understand their function. However, up to now only information about the supramolecular assembly of a GPR variant have been obtained using atomic force microscopy and electron microscopy [8,9]. Additional insights result from the chemical shift analysis of solid state NMR data [10,11]. Here protonation states of several carboxylic acids as well as boundaries and distortions of transmembrane α -helices and secondary structure elements in the loops could be identified. However, the structure on an atomic level still remains unresolved. Nevertheless, specific structural insights could be obtained by spectroscopic methods [12–19] and homology modeling to bacteriorhodopsin (BR) [1,2,20] and sensory rhodopsin II (SRII) [21]. It could be shown that all key residues involved in the vectorial proton transfer in BR such as the primary proton donor (BR: Asp-96; PR: Glu-108), the proton acceptor group (BR: Asp-85, Arg-82, Asp-212; PR: Asp-97, Arg-94, Asp-227) and the Schiff base linking via a lysine residue (BR: Lys-216; PR: Lys-231) are functionally conserved. Nevertheless, notable differences between the archaeal BR and the microbial PR have been identified. Amongst those the unusually high pK_a value (7–8) of the primary proton acceptor (Asp-97) is the most striking one [14,22]. A highly conserved His residue also found for the eubacterial proton pump xanthorhodopsin (XR) [23] is discussed to contribute to this property via an Asp-His counterion complex [24–26], but it is likely that the His does not exclusively account for the high pK_a value. Concomitant with the protonation state of Asp-97 the proton pumping direction changes dependent on pH [14,27]. At alkaline pH

Abbreviations: BR, bacteriorhodopsin; BPR, blue-absorbing proteorhodopsin; GPR, green-absorbing proteorhodopsin; PR, proteorhodopsin; PR rec., reconstituted proteorhodopsin sample; PR 2D, 2D crystallized proteorhodopsin sample; SRII, sensory rhodopsin II; XR, xanthorhodopsin

* Corresponding author. Tel.: +49 69 798 46410; fax: +49 69 798 46423.

** Corresponding author. Tel.: +49 69 798 29351; fax: +49 69 798 29709.

E-mail addresses: maentele@biophysik.uni-frankfurt.de (W. Mäntele),

wachtveitl@theochem.uni-frankfurt.de (J. Wachtveitl).

¹ These authors contributed equally to this work.

values outward proton flow is observed as in BR, associated with the appearance of five distinct photocycle intermediates, which were termed K, L, M, N, O states [14,19,22,28,29]. On the contrary, inward pumping is observed under acidic conditions [14,27]. This vectorial proton transport has been discussed controversially over the last decade for two main reasons. First, the inversion of the pumping direction could not be confirmed by photocurrent measurements of oriented membranes by Dioumaev et al. [13], and second only red-shifted intermediates have been identified spectroscopically under acidic pH conditions [14,30]. The so called M state, which is thought to represent the switching process in BR and is also a key feature of the inward pumping mechanism proposed by Friedrich et al. [14], is kinetically absent. However, recent two-electrode voltage-clamp experiments on PR-expressing *Xenopus* oocytes under different acidic pH conditions have confirmed the inward-directed proton transport. Additionally, low-temperature spectroscopy in the visible spectral range could show the undisputable occurrence of a M-like species at low pH [27]. Also a fluorescence essay supports the bidirectional pumping mechanism [25].

2. Materials and methods

2.1. Proteorhodopsin expression

Expression and purification were performed as described in Neumann et al. [31]. The protocols for reconstitution (PR rec.) and crystallization (PR 2D) are given in references [18] and [9], respectively. Measurements were performed in 100 mM phosphate buffer containing 100 mM NaCl.

2.2. Low temperature FTIR spectroscopy

For the low-temperature measurements a hydrated film sample was prepared between two flat CaF_2 windows. For this purpose a high concentrated protein solution was put on one CaF_2 window and dried at room temperature for 20 min. The film was rehydrated and the second CaF_2 window was placed on top of the film resulting in a film thickness of approx. 5 μm . The film preparation was controlled by taking both UV–visible and FTIR absorbance spectra, observing water bands, amide I and II absorption and the electronic spectrum arising from the chromophore. These controls ensure reproducible and functionally intact PR samples. The ratio of the amide I/amide II bands indicated that these films were not oriented. The light-minus-dark spectra were collected on a modified Bruker IFS66 spectrometer using a liquid N_2 -cooled cryostat (OptistatDN, Oxford Instruments, Oxfordshire, UK). Data were collected from 1150 to 2000 cm^{-1} with a resolution of 4 cm^{-1} . The samples were illuminated for 60 s by a mercury-xenon lamp (LC 8-04, Hamamatsu Photonics, Herrsching, Germany) with a bandpass filter combination (Thorlabs, Karlsfeld, Germany) to select the 500–550 nm range of the spectrum.

2.3. Low temperature visible spectroscopy

A home built fiber UV–visible spectrometer (200 nm – 800 nm) was implemented in the FTIR spectrometer at a tilt angle of 10° with respect to the IR beam. A combined deuterium-halogen lamp (DH-2000, Micro-pack Inc., Ostfildern, Germany) served as light source. The light was coupled into the cryostat using a quartz fiber with 100 μm core diameter (Avantes, Eerbeek, the Netherlands) equipped with collimating and focusing optics. For detection a MCS 55 multichannel spectrometer module (Carl Zeiss, Oberkochen, Germany) was utilized. The spectra were collected with 300 ms integration time, ten scans were averaged. The empty cryostat was used as reference for the calculation of the absorbance spectra. Illumination of the sample was provided by the same setup as described in the IR part. In order to correct for light scattering in the raw spectra, a power function ($A + B \cdot \lambda^{-C}$) was subtracted and difference spectra ($\text{PR}_{\text{illuminated}} - \text{PR}_{\text{dark}}$) were calculated.

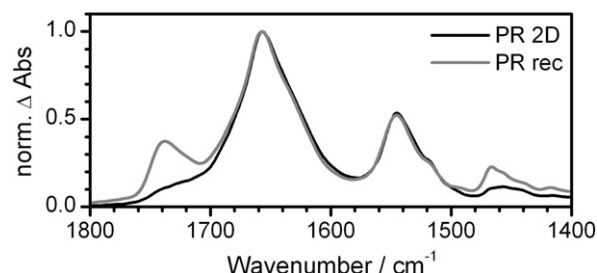


Fig. 1. IR absorption spectra of 2D crystallized (black) and reconstituted (gray) PR films. The PR 2D sample contains a significant smaller amount of lipids (band at 1740 cm^{-1}).

3. Results

The aim of this study is the further characterization of the low-pH photocycle of PR. To get insights into the proton translocation steps and concomitant helix movements the structure sensitive method of FTIR spectroscopy is used. Since it was demonstrated that nearly the complete photocycle transitions of acidic PR can be resolved at low temperatures [27] the measurements were performed under these conditions.

For this purpose sample films with a water/amide I band to amide II band ratio of ~2:1 were prepared. Sodium phosphate was selected as IR-compatible buffer system due to the lack of bands between 1150 cm^{-1} and 1800 cm^{-1} . The measurements were performed at pH 5.1 and 5.5. Earlier studies have demonstrated that besides the water content also the amount of lipids as well as the type of added lipids strongly influence the photocycle kinetics of retinal proteins [32,33]. For this reason protein films of two different sample preparations, i.e. reconstituted PR (PR rec.) and 2D crystallized PR (PR 2D) were tested. For both preparations time-resolved spectroscopy could show the appearance of all signatures expected for an active protein with only slightly altered kinetic properties depending on the lipid contents [14,34]. We take this fact as a proof for functional integrity. However, the PR 2D protein films possess a significantly higher stability. Additionally, they have the advantage of a lower lipid content (protein-lipid-ratio of 0.25 (w/w), Fig. 1), leading to reliable signals in the spectral region above 1700 cm^{-1} where the protonation changes of the side chains of Asp and Glu are monitored. The PR 2D sample was therefore chosen for the present study.

3.1. Photoisomerization at 77 K

Fig. 2 shows the light-induced difference spectrum of acidic PR at 77 K. The peak pattern found in this spectrum resembles the PR difference spectra obtained at the maximal delay time (~2 ns) of pump probe measurements (region of the C–C, C=C and the C=N stretching vibration of the chromophore) [12,31,35]. It can therefore be concluded

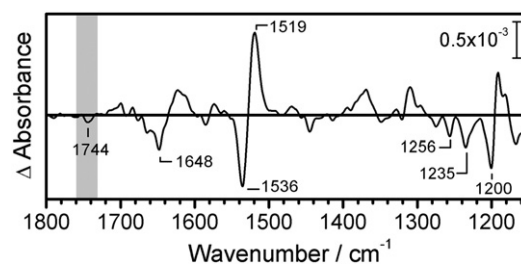


Fig. 2. Light-induced difference spectrum of a PR 2D sample buffered at pH 5.1 recorded at 77 K. The main signals stem from the depleted ground state (negative bands) and the formed PR_K intermediate (positive bands). The negative signature at 1744 cm^{-1} indicates also an additional contribution of the PR_L state.

that the product bands of the difference spectrum mainly stem from the first photocycle intermediate, PR_K . In reference to BR and already published low temperature FTIR data [16,36] the following band assignments can be made: Between 1180 cm^{-1} and 1260 cm^{-1} the difference pattern of the C-C stretching vibration of the chromophore is found. The positive bands at 1182 cm^{-1} and 1192 cm^{-1} in combination with the negative bands at 1200 cm^{-1} , 1235 cm^{-1} and 1256 cm^{-1} bear the typical signatures of the all-*trans* to 13-*cis* isomerization of the retinal. The N-H and the C-H in-plane vibrations are present around 1360 cm^{-1} – 1390 cm^{-1} and 1290 cm^{-1} – 1320 cm^{-1} , respectively. At $(-)$ 1536 cm^{-1} the C=C stretching vibration of the depleted all-*trans* retinal chromophore is observable. The C=C stretching band of the 13-*cis* photoproduct is located at $(+)$ 1519 cm^{-1} . Since the chromophore absorption maximum in the visible and the position of the C=C stretching vibration are correlated in retinal proteins (-4 nm/cm^{-1}) [37,38] the position of the bleached C=C stretching vibration shows a small pH dependence (pH 9.0: 1540 cm^{-1} , pH 5.1: 1536 cm^{-1}). It can therefore serve as internal pH marker. The difference signature in the spectral range between 1500 cm^{-1} and 1550 cm^{-1} most likely contains additional small contributions of local amide II changes, as shown by Amsden et al. in ultrafast transient absorption measurements of reconstituted PR at pH 9.5 [12]. The C=N stretching vibration of the Schiff base retinal chromophore link can be found around 1650 cm^{-1} [15,16]. In this region also first local amide I changes are monitored [31,36]. A small difference signature is observed at $(-)$ 1693 cm^{-1} / $(+)$ 1702 cm^{-1} . It has been attributed to a perturbation of Asn-230 [36]. In addition, a further clear negative signal is observed at 1744 cm^{-1} . This band has been neither observed in light-induced difference spectra of alkaline nor of acidic PR samples at 77 K before, which might be due to different lipid concentrations. The band position favors the interpretation of an isomerization-induced perturbation of a carboxylic side chain of an Asp or Glu residue as it was found for the BR_L intermediate [39,40].

The described difference pattern of the first intermediate can be trapped (which means that no time-dependent evolution of the bands is observed) up to temperatures of about 190 K. This is most likely connected to the protein-solvent glass transition, which results in the arresting of surface-coupled rotational and librational degrees of freedom, whereas internal protein modes as rotations of side chains or in this case the isomerization of the chromophore are unaffected [41]. Above 190 K the light-induced difference spectra are not static any more. For the characterization of the subsequent photocycle intermediates we therefore used time-resolved rapid scan IR spectroscopy. This technique allows following the time course of the difference bands as well as the calculation of difference spectra at certain times after illumination. At a temperature of 242 K nearly the full photocycle transitions can be observed within a recording time of 1 hour. Transient absorbance changes indicating the K decay (C-C and amide II/C=C stretching region) are displayed in Fig. 3A and B. In Fig. 3C–E the time course of the bands assigned to the C=N stretching vibration of the retinal chromophore and the amide I changes (C) as well as the small but reproducible temporal characteristics of the carboxylate vibrations (D and E) are shown.

3.2. Photocycle dynamics at 242 K

At 242 K, the first spectrum after excitation (Fig. 4A) shows mainly the prominent features of the PR_K -PR difference spectrum as discussed in the paragraph above. Nevertheless, it differs from the one recorded at 77 K (Fig. 2) in the spectral region of the carboxylate vibrations ($>1700\text{ cm}^{-1}$). Instead of the negative signature at 1744 cm^{-1} , a positive contribution around 1730 cm^{-1} is observed. In general, this positive band is visible in the early difference spectra recorded at temperatures $>200\text{ K}$. It can most likely be attributed to a protonation of an Asp or Glu side chain.

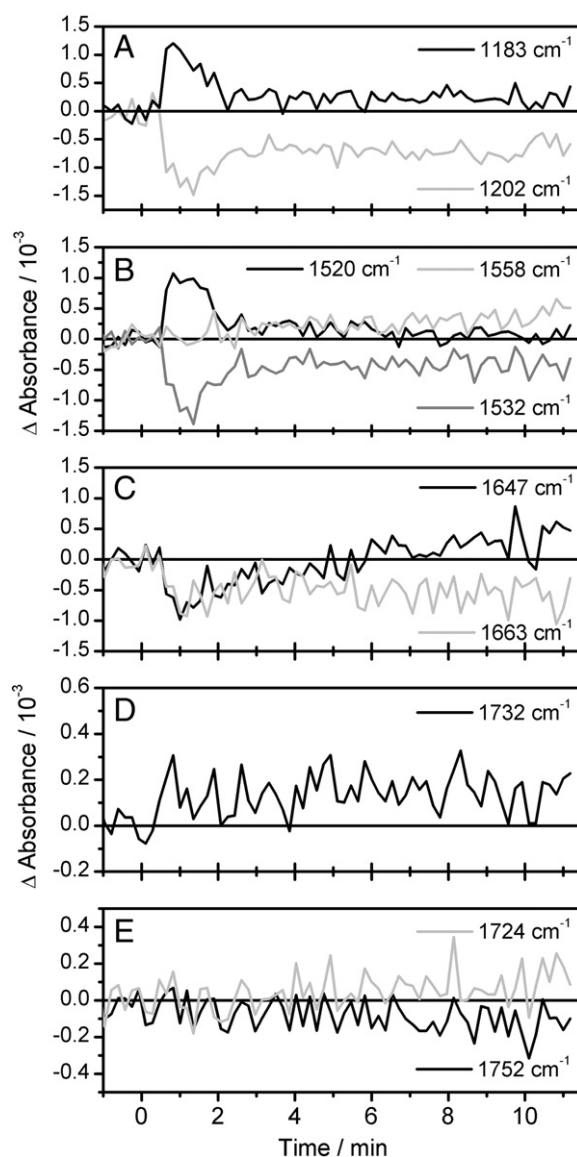


Fig. 3. Transient absorbance changes of PR 2D at pH 5.1 recorded after 1 min illumination at 242 K. (A) and (B) depict the time evolutions of the bands in the region of the C-C and the C=C stretching vibrations of the chromophore. The time courses at 1647 cm^{-1} and 1663 cm^{-1} (C) reflect the light-induced changes of the C=N stretching vibration band which are superimposed by the formation of strong amide I difference bands. The transients at 1732 cm^{-1} (D), 1724 cm^{-1} and 1752 cm^{-1} (E) are directly linked to the protonation or deprotonation kinetics of Asp or Glu side chains.

As illustrated in the transient absorbance changes for individual wavenumbers (Fig. 3D), the protonation signature at 1732 cm^{-1} stays constant during the next 10 min, whereas the contributions of the C-C and C=C stretching vibrations around 1200 cm^{-1} and 1530 cm^{-1} decay on a 2 min time scale (Fig. 3A and B). The band at 1520 cm^{-1} thereby reaches zero around 7 min after excitation. Also the negative signals in the region of the C=N stretching region decay on this time scale (Fig. 3C).

The overall decrease of the PR_K -PR difference pattern leads to a difference pattern for $t = 3\text{--}4\text{ min}$ with a remarkably small amplitude in the range of 0.5×10^{-3} (see Fig. 4B). The signal to noise ratio is therefore lower compared to the other spectra. At times $>4\text{ min}$ the difference signals start to grow again. The biggest changes are monitored in the amide I region. The initially negative absorbance change at 1647 cm^{-1} changes sign after 6 min and further grows to positive absorbance changes, whereas the signal at 1663 cm^{-1} turns again

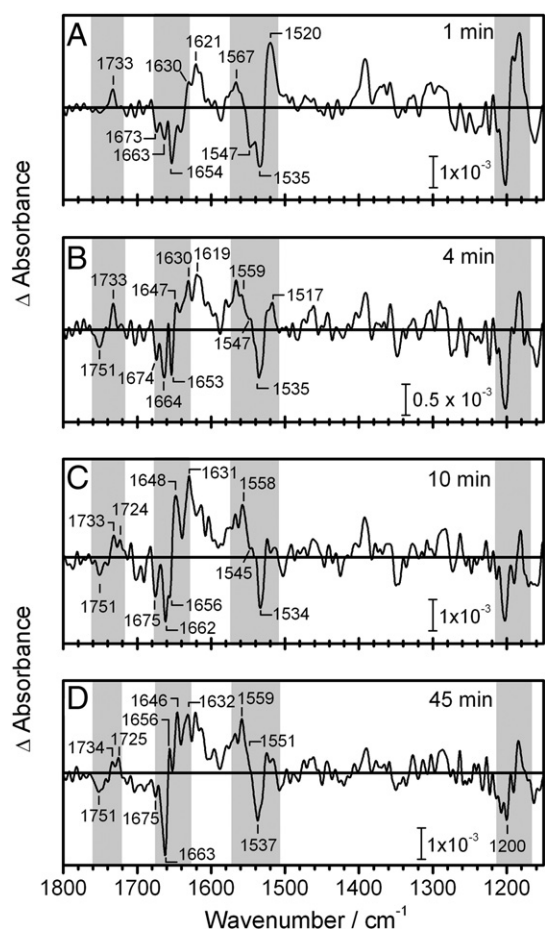


Fig. 4. Transient light-induced spectra of PR 2D at pH 5.1 recorded at 242 K. The first three spectra (A–C, 1 min, 4 min and 10 min after excitation) are taken from a rapid scan experiment. The spectrum 45 min after excitation (D) is from a static measurement after the rapid scan.

negative (Fig. 3C). At the same time a positive contribution arises around 1560 cm^{-1} (Fig. 3B). This signal can be most likely assigned to the amide II mode and/or the $\text{C}=\text{C}$ stretching vibration of the subsequent intermediates. Also in the carboxylate region new difference bands evolve on this time scale. Around 1750 cm^{-1} a negative signature is observed. A positive band around 1720 cm^{-1} is formed somewhat delayed. Both difference bands further grow in the next minutes and reach their maximum 45 min after excitation. An exemplary difference spectrum for this time is depicted in Fig. 4D.

3.3. Assigning the difference signatures to the intermediates of the photocycle

After careful consideration, the difference signals recorded at certain times in the reaction cycle can be attributed to one intermediate or to a mixture of different intermediates. A clear cut band assignment of the $\text{PR}_{\text{K/L}}$ -PR difference spectrum can be obtained from the spectra measured at 77 K. Besides the negative band at 1744 cm^{-1} all features are well known and understood [16,36]. It can also be assumed that the spectra recorded 45 min after excitation at 242 K should neither have significant contributions of the early K state, since these decay within the first minutes after excitation (see Fig. 3A and B), nor of the M intermediate, because only a small amount of M should be present at this temperature [27]. The difference spectra therefore most likely show a mixture of the N/O-like states. Due to the low signal to noise ratio the spectra of the N and O state cannot be disentangled from the recorded data by fitting a kinetic model.

To visualize the contribution of the M intermediate, visible and IR difference spectra were simultaneously monitored. This approach allows the direct identification of the M state due to the characteristic blue shifted absorption band in the visible spectral range ($\lambda_{\text{max}}(\text{M}) = 420\text{ nm}$), which is clearly separated from the other intermediates ($\lambda_{\text{max}}(\text{N/O}) \geq 540\text{ nm}$). For this purpose measurements in the visible and IR were performed at 237 K since at this temperature the strong difference bands observed at the end of the reaction cycle (see Fig. 4C and D) are not present.

An exemplary set of two difference spectra recorded in the IR and visible is presented in Fig. 5. The spectra were taken at 1 min after excitation at 237 K. In the IR, the already discussed signature of the $\text{PR}_{\text{K/L}}$ -PR spectrum is the dominant feature in the spectral region between 1150 cm^{-1} and 1700 cm^{-1} . An altered band shape in the region of the $\text{C}=\text{C}$ stretching vibration probably points to beginning amide II contributions at 237 K. In contrast to the $\text{PR}_{\text{K/L}}$ -PR difference spectra recorded at 77 K, where a negative signature is observed above 1700 cm^{-1} , a positive signature at 1728 cm^{-1} is visible in the early spectra at 237 K. The signal must be due to the protonation of an Asp or Glu side chain. The observed red shift of the band compared to the measurement at 242 K (1733 cm^{-1}) should be due to the different temperature conditions. This is supported by the fact that the band further shifts to 1722 cm^{-1} at 227 K (compare Figs. 4A, 5A and 7C). The respective difference spectrum in the visible shows the negative signature of the depleted ground state at 530 nm and two positive photoproduct signals at 420 nm and 600 nm. Due to the pronounced PR_{K} marker bands in the IR difference spectrum, the band around 600 nm can be ascribed to PR_{K} . The second product band in the visible difference spectrum at 420 nm must be unambiguously assigned to the M state. To estimate the fraction of the M state observed in the difference spectrum depicted in Fig. 5B the percentage of PR_{M} and PR_{K} was calculated adopting the extinction coefficients of BR and its K and M intermediate [42] to the known extinction coefficient of ground state PR at pH 4 ($\epsilon = 45,000\text{ M}^{-1}\text{ cm}^{-1}$) [14]. The yields of PR_{M} and PR_{K} are approximately 40% and 60%, respectively.

Subsuming, it can be stated, that the deprotonation of the Schiff base (as evidenced in the visible difference spectrum) consequences the protonation of an Asp or Glu side chain (as observed in the IR difference spectrum). Unfortunately, the deprotonated Schiff base signature cannot be easily resolved in IR measurements.

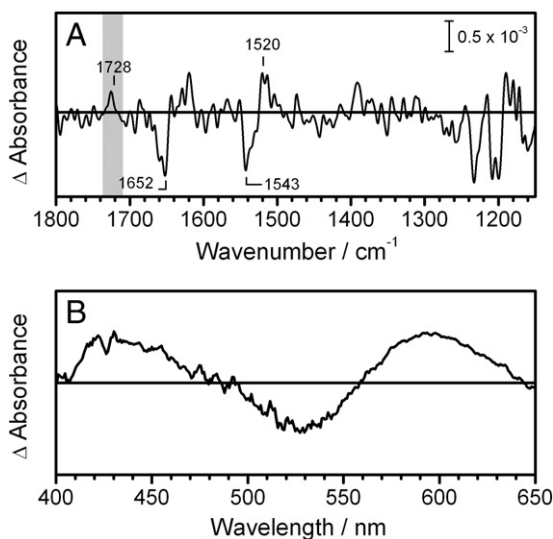


Fig. 5. FTIR difference spectrum (A) simultaneously recorded with the visible difference spectrum (B) for the pH 5.1 sample at 237 K, 1 min after excitation. The combination of the carboxylate signal at 1728 cm^{-1} and the prominent difference signal at 420 nm is indicative for an M-like intermediate.

3.4. Temperature dependence of the frequency of the primary proton acceptor

The comparison of the early light-induced spectra taken at 242 K, 237 K and 227 K shows that the band position of the positive protonation signal of the primary proton acceptor exhibits an unusual blue shift with rising temperature (compare Figs. 4A, 5A and 7C). These characteristics are observed for 2D crystallized as well as reconstituted PR samples. To substantiate this finding further spectra taken at temperatures below and above these were evaluated (Fig. 6). Indeed, at a temperature of 212 K the protonation signature of the proton acceptor further downshifts to a wavenumber of 1719 cm^{-1} . Below this temperature the positive band is very small or not observed. Instead, the difference spectra in the region of the carboxylate signals are dominated by a negative band around 1740 cm^{-1} , which was also monitored in the spectra taken at 77 K (Fig. 2). For temperatures $>250\text{ K}$ the evaluation is challenged by the fact that the de-/protonation signatures of the different carboxylic side chains cannot be temporally separated. Nevertheless, besides bands at $(+)$ 1721 cm^{-1} and $(-)$ 1752 cm^{-1} the early light-induced difference spectra of acidic PR samples exhibit a positive band at 1744 cm^{-1} , which is most likely due to the protonation of the proton acceptor. At a temperature of 257 K the difference pattern at $(+)$ $1744\text{ cm}^{-1}/(-)$ 1752 cm^{-1} exhibits a considerably smaller amplitude compared to the one at 250 K, which most likely hints to the fact that both signals superimpose each other.

3.5. Influence of small pH changes on the PR photocycle

Previous electrophysiological experiments have proven that in PR directed proton transfer takes place at pH values higher than 9 and lower than pH 5 [14,27]. Nevertheless, there is an ongoing discussion about the active proton transport at different pH values in the literature, especially at low pH. We therefore additionally studied the PR photocycle at a pH value 0.4 pH units further to the pK_a of Asp-97 (pH 5.5).

Fig. 7A displays the difference spectra obtained at 77 K for the two selected pH values. All key features of the all-*trans* to 13-*cis* isomerization including the pH-dependent shifting of the C=C stretching band are present at pH 5.5. Also the negative carboxylate signature at 1744 cm^{-1} is observed at this pH value. Besides these similarities, one small difference is observed around 1540 cm^{-1} . Here, the spectrum at pH 5.5 exhibits an additional shoulder, which overlaps with the C=C stretching difference pattern of the $PR_{K/L}$ -PR spectrum. The band position argues for a local amide II contribution.

Also for the subsequent photocycle intermediates and transitions pH-dependent differences are observed. The availability of time-resolved data enabled us to identify not only spectral differences, but also altered reaction dynamics. As an example for the latter point the comparison of the K decay monitored by the decay of the C=C stretching vibration of the PR_K state at 227 K is presented in Fig. 7B. In the time range of 1–2 min fast decay kinetics are found

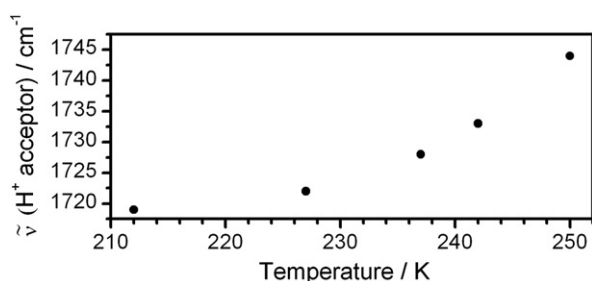


Fig. 6. Temperature-dependence of the band position of the primary proton acceptor. The values are taken from different rapid scan experiments recorded after 1 min illumination.

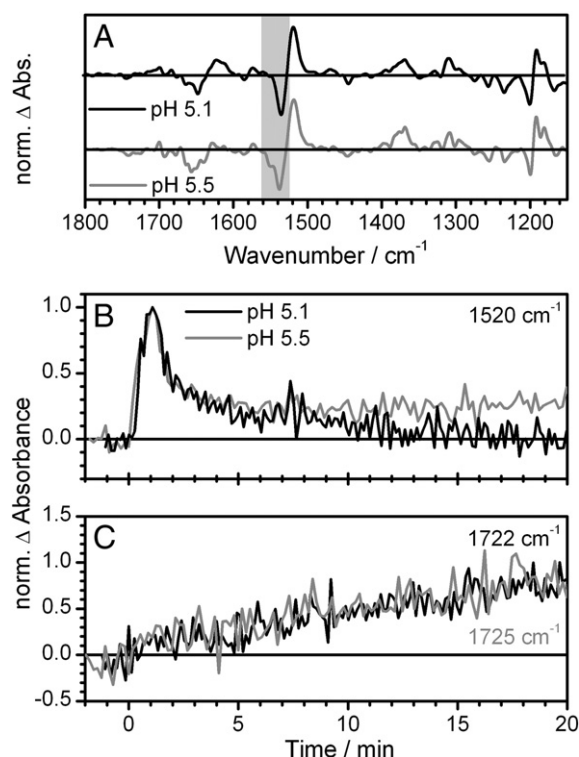


Fig. 7. A: Comparison of the light-induced difference spectra of acidic PR samples (pH 5.1 = black, pH 5.5 = gray) at 77 K. A significant difference between both spectra is observed around 1540 cm^{-1} , where an additional shoulder is observed at pH 5.5. In B and C transient absorbance changes of PR recorded at 227 K are shown. A clearly different dynamics is observed for the decay of the K state (1520 cm^{-1}), whereas the protonation kinetics of the proton acceptor ($1722\text{ cm}^{-1}/1725\text{ cm}^{-1}$) is equal within the signal to noise ratio.

for both samples. But whereas the signal at pH 5.1 decays nearly to zero, the one at pH 5.5 reaches a plateau after several minutes. For pH 5.5, a higher amount of $PR_{K/L}$ should therefore be present in the subsequent equilibrium of states. However, the protonation kinetics of the primary proton acceptor residue (Asp or Glu) is not affected by the pH as can be seen in the normalized transient absorbance changes at $1722\text{ cm}^{-1}/1725\text{ cm}^{-1}$ in Fig. 7C.

The influence of the small pH change to the difference signals is most pronounced at the end of the reaction cycle (Fig. 8, 242 K, 45 min after excitation). The difference signals in the whole spectral range are less pronounced at pH 5.5. In the amide I region, the most prominent pair of a negative and a positive band at pH 5.1 ($(-)$ 1663 cm^{-1} , $(+)$ 1646 cm^{-1}) is even completely missing at pH 5.5. Only the difference bands at $(-)$ $1674\text{ cm}^{-1}/(+)$ 1659 cm^{-1} are present. In addition, the negative signature at 1751 cm^{-1} is absent in the difference spectrum at pH 5.5.

4. Discussion

In this paper an elaborated characterization of the low pH photocycle of PR is presented. The inherent structural sensitivity of IR spectroscopy thereby allows following the individual proton translocation steps. Due to the variable temperature conditions the different parts of the photocycle could be addressed either separately or at an elongated time scale (compared to room temperature) one after another. As a consequence the altering Asp/Glu side chain protonation states could be ascribed to certain time points in the reaction cycle. According to the obtained results the photocycle of PR at pH 5.1 can be described as follows:

The spectrum at 77 K is dominated by the light-induced changes of the retinal chromophore. Besides the expected small shift of the

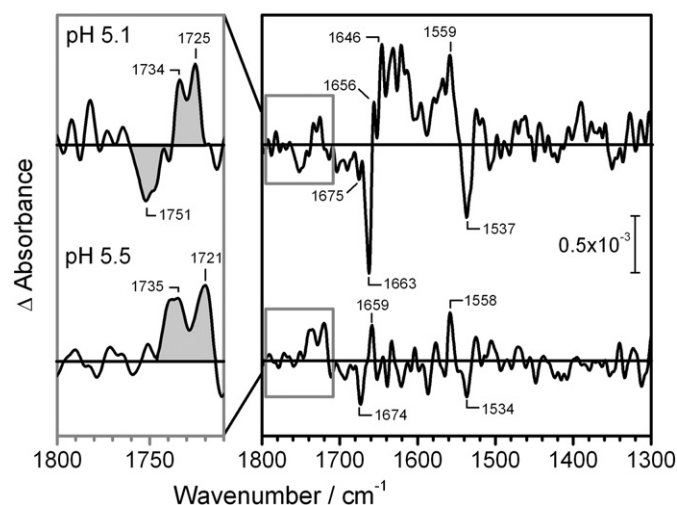


Fig. 8. Transient difference spectra of PR at pH 5.1 (top) and pH 5.5 (bottom) recorded 45 min after illumination at 242 K. The spectral region between 1800 cm^{-1} and 1710 cm^{-1} , where the characteristic protonation changes of the Asp and Glu side chains are monitored, is enlarged in the left panel. The negative deprotonation signature observed at pH 5.1 is absent in the trace of the pH 5.5 sample. Also the strong amide I and amide II changes are much less pronounced at pH 5.5; the difference pattern absorbing at (–)1663 cm^{-1} /(+)1646 cm^{-1} is even completely missing.

C = C stretching vibration of the depleted ground state, the observed chromophore difference bands are at the same position for pH 9.0 and pH 5.1 [15,16,36]. It can therefore be assumed that the retinal chromophore fulfills a proper all-*trans* to 13-*cis* isomerization at the acidic pH value. Small local amide I and amide II contributions are thought to be present around 1650 cm^{-1} as well as around 1540 cm^{-1} [12,31]. A perturbation of an Asn side chain is discussed to cause the difference signature around 1700 cm^{-1} [36]. The difference spectra additionally show a negative signature at 1744 cm^{-1} , which is only present at low pH. However, up to now this signal has not been monitored in other low temperature FTIR spectra at 77 K [15,36]. Though, step-scan measurements of PR reconstituted into dimyristoylphosphatidylcholine vesicles at pH 9.5 by Xiao et al. revealed a strongly pH-dependent band at 1740 cm^{-1} which emerges during the K state decay [19]. A negative signature in this spectral region has also been observed in the early steps of the BR photocycle. Here, the signal is attributed to the disturbance or deprotonation of the primary proton donor Asp-96 [39,40] and is used as indicator for the BR_L state. In analogy to BR, the observed negative signature at 1740 cm^{-1} in our PR difference spectra could be assigned to the perturbation of a homologous amino acid in PR. We excluded that the band originates from the lipids in the sample, because first the band is only formed at low pH (data for pH 9.0 not shown) and second it is built to the same extent regardless of the lipid concentration (data for PR rec. not shown). For all stated reasons, we term the difference spectrum measured at 77 K a PR_{K/L}-PR spectrum.

The decay of the K/L state can be monitored at temperatures higher than ~200 K. This is most likely due to the protein glass transition, which is discussed to occur around 180 K for protein films [41]. The difference spectra now exhibit a very low amplitude. Besides the residual difference pattern of the PR_K state, a new positive signature is observed in the region of the carboxylate vibrations. This band is strongly temperature dependent and shifts from 1733 cm^{-1} at 242 K to 1728 cm^{-1} at 237 K and 1722 cm^{-1} at 227 K (Fig. 6). This might be interpreted in a way that either the microenvironment of this Asp or Glu residue or its conformation drastically changes with temperature. However, we have to point out, that we cannot be sure whether this signature is associated to one single side chain. The possibility to record IR and visible spectra at the same time enables us to identify that the observed protonation of an Asp or Glu

side chain, manifested by the positive band around 1728 cm^{-1} , is the consequence of the deprotonation of the Schiff base (M intermediate), which is sensed by the difference band at 420 nm in the visible spectrum (Fig. 5). This shows that the proton translocation pathway at pH 5.1 also proceeds via the Schiff base. The band position in the IR shows that the proton acceptor at this pH value must be an Asp or Glu. There are in principle three Asp and Glu residues within the retinal binding pocket. Asp-97 and Asp-227 are in the immediate vicinity of the Schiff base. According to the homology model [20] the carbons of both carboxylate groups are 5 Å away from the nitrogen of the Schiff base. Yet, Asp-97 cannot be the proton acceptor since it should be already protonated at pH 5.1. The pK_a of Asp-227 was reported to be around 2.5 [43,44], making Asp-227 a likely candidate. However, the protonation signature of the analogous residue in BR, Asp-212, is found at a significantly lower frequency (1712 cm^{-1}) [45–47]. This may be explained by a different environment (H-bonding network, charge distribution) of both residues. Taking the inversion of the pumping direction at acidic pH into account [27] Glu-108 could also be the proton acceptor. The exact pK_a of Glu-108 is to our knowledge unknown, but since Glu-108 functions as proton donor at pH values higher than the pK_a of Asp-97, Friedrich et al. suggested a value above 10 [14]. For the homologous residue in BR, Asp-96, the pK_a value was determined to be ≥10 [48,49]. The carboxyl side chain of Glu-108 is within 11 Å distance from the Schiff base nitrogen. An auxiliary water cluster must therefore be present between both residues to assist a possible proton transfer. For BR a water cluster between the homologous residue Asp-96 and the Schiff base has been demonstrated [50].

The formation of the positive signature at around 1728 cm^{-1} is followed by drastic changes in the amide I and II region. The altered band shape in the amide II region of the very early spectra at 237 K and 242 K compared to the 77 K difference spectra already indicates first backbone movements. The emerging amide difference bands are developed to their full extent at the end of the reaction cycle (242 K, $t > 30$ min), where most likely the N- and O-like late intermediates are present. The most prominent feature in this FTIR difference spectrum (Fig. 4D) is a pair of a negative and a positive band in the amide I region ((–)1663 cm^{-1} , (+)1646 cm^{-1}). A second difference band smaller in intensity ((–)1675 cm^{-1} , (+)1656 cm^{-1}) is also present in this region. In accordance to BR, where a strong difference band at (–)1670 cm^{-1} /(+)1650 cm^{-1} was found in the N intermediate difference spectra, these difference bands are attributed to backbone movements of the peptide carbonyl groups [51]. The signal next in size in the spectrum is found in the C = C stretching/amide II region. Besides the bleached ground state C = C stretching signature ((–) 1537 cm^{-1}), two positive contributions at 1551 cm^{-1} and 1559 cm^{-1} are found. These signals must be either due to amide II changes or the C = C stretching vibrations of PR_N. The C = C stretching signal of the PR_O state is expected to be red shifted ((+) 1520 cm^{-1}) to the depleted ground state band. Indeed a positive signature in this spectral region is monitored at very long observation times.

The structural movements are attended by protonation changes of two further carboxylic residues. The formation of a negative signature at 1751 cm^{-1} is somewhat faster observed as the rise of a positive signal at 1724 cm^{-1} (Fig. 3E). Also in BR, a negative signal is monitored in the carboxylate region at the end of the reaction cycle (N intermediate). It is attributed to the transient deprotonation of the proton donor, Asp-96 [40,46]. For PR at pH 5.1, the band position of the negative signal at 1751 cm^{-1} matches the positive protonation signal of Asp-97 at alkaline pH [14,19,22]. This may favor an interpretation in terms of transient deprotonation of Asp-97 at the end of the PR photocycle at pH 5.1. Nevertheless, it can also not be excluded that another Asp or Glu side chain is deprotonated since the shift of the resonance frequency in different photocycle intermediates is also known from BR. Moreover, a possible assignment of the positive signature at 1724 cm^{-1} is the protonation of Asp-227. As stated above,

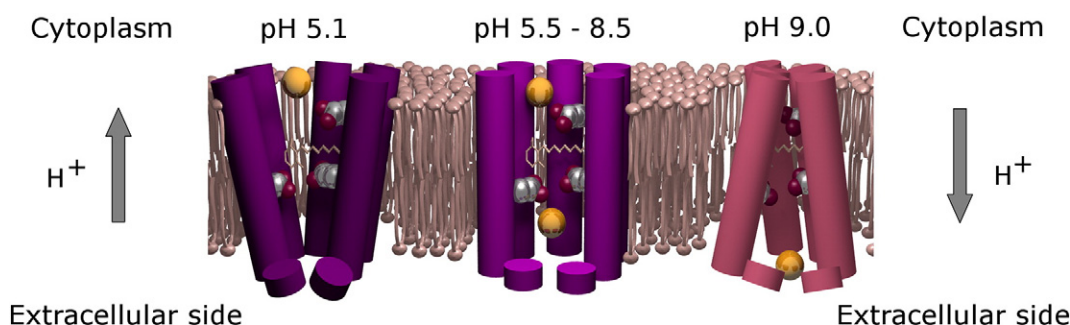


Fig. 9. Schematic picture of the proposed mechanism for the proton translocation in PR. There are three pH-dependent states for the protein. In accordance with already published data at pH 9 outward directed proton pumping takes place. Between pH 8.5 and 5.5, around the pK_a of the key amino acid Asp97, no large protein motions occur and therefore no directed proton transport is proposed. At pH 5.1 the system starts working again and is able to pump protons inwards.

this residue should exist in its deprotonated form (pK_a of 2.5 in the ground state [43]) unless it has not been protonated at the beginning of the reaction cycle. For BR it was shown that the H-bonding pattern of the analogous residue Asp-212 is crucial for the proton transfer [52]. An attribution to a release complex (most probably composed of Glu-245, Glu-50 and/or Asp-52 taking the inversion of the proton pump direction into account) is rather unlikely, since in BR difference bands of the release complex of Glu-194 and Glu-204 have not been detected in time-resolved FTIR experiments [53,54]. This finding was referred to a hydrogen bonded network in the extracellular channel comprising Asp-85, Arg-82, the dyad of Glu-194 and Glu-204 [53,55] as well as intervening water molecules [50,56,57]. Last but not least, the negative/positive signature at $(-)/1751\text{ cm}^{-1}/(+)/1724\text{ cm}^{-1}$ could also be due to a spectral red shift of an Asp or Glu C=O vibration which would lead to a negative band in the region of the initial frequency and a positive band red shifted to this frequency.

To further examine the pH sensitivity of the PR photocycle additional measurements were performed at a pH value 0.4 units closer to the pK_a of Asp-97. Already the $PR_{K/L}$ -PR difference spectra of both samples (77 K, Fig. 7A) have shown distinct variations in the region of the C=C stretching vibration. Here an additional shoulder is observed for PR at pH 5.5. Since in this spectral region amide II changes are expected, the monitored shoulder can be attributed to first local structural changes. This means that the reaction barriers for the transition to the subsequent intermediates, including conformational changes, are lowered at pH 5.5.

Altered photocycle properties of PR at pH 5.1 and 5.5 are also evident in the further reaction steps. The two most outstanding features are discussed in the following. First, the transient absorbance changes of the C=C stretching vibration of the K photoproduct (227 K) are presented (Fig. 7B and C). The traces of both samples show a decay kinetics on a 1–2 min time scale. But whereas the signal at pH 5.1 reaches zero, a residual signal persists at pH 5.5. This could on the one hand hint to a significantly elongated life time of the K state at pH 5.5. On the other hand, the positive offset signal may also be traced back to the C=C stretching vibration of a red-shifted late intermediate. However, the formation of the protonated proton acceptor is not influenced by the small pH changes as can be seen in the transients in Fig. 7C. This protonation kinetics might therefore correlate with the first pH independent decay of the K state. As a second example for the influence of small pH changes the difference spectra of the late photocycle steps (45 min, 242 K, Fig. 8) are compared for pH 5.1 and 5.5. The overall difference amplitude at pH 5.5 is drastically smaller than at pH 5.1. It is particularly noticeable that the prominent difference pattern in the amide I region $(-)/1663\text{ cm}^{-1}/(+)/1646\text{ cm}^{-1}$ is missing at pH 5.5. This hints to the fact that in this case fewer changes in the protein structure are observed at the end of the photocycle. At pH 5.5, also the negative signature of the deprotonated Asp or Glu side chain at $(-)/1751\text{ cm}^{-1}$ is absent in the difference spectrum. Different proton translocation pathways are therefore active at both pH values.

Thus, the question arises, whether directional proton pumping can be established at all at this pH value.

A comparison of low temperature FTIR spectra at pH 8.5 and 9.0 also revealed several differences in the photocycle, which are not further discussed here. All available data on the influence of small pH changes on the PR photocycle validate the fact that the functional properties of PR are not only determined by the pK_a value of the primary proton acceptor, but the interplay of several pH-sensitive equilibria of protonation/deprotonation steps connected with rearrangements in the hydrogen bonding network. Part of the changes can be attributed to structural rearrangements in the binding pocket due to a protonation change of His-75. The direct involvement of His-75 in the hydrogen bonding network of PR could recently be demonstrated by NMR [24,25] as well as visible and FTIR [26] studies. For the related bacterial rhodopsin XR the participation of an analogous residue in the counterion complex has been shown [23].

Based on our data we propose a three-state model (Fig. 9) that explains the complex pH dependence of PR. At pH 9.0 the photocycle of PR is BR-like and the active proton transport is undisputed. The data recorded at pH 5.1 show a full photocycle with an altered proton acceptor. Lörinczi et al. demonstrated that under these conditions the vectoriality of the H^+ transport is inverted and protons are pumped into the cytoplasm [27]. Compared to the pH values at which active proton pumping is observed, our data measured on PR at pH 5.5 and 8.5 (not shown) show drastic changes concerning the backbone movements and the protonation/deprotonation steps. This might implicate that near the pK_a of Asp-97 directed proton pumping is not established at all. This assumption is substantiated by the fact that Dioumaev et al. reported a dramatic decrease in the proton transport activity between pH 9.0 and pH 8.5 [13].

Acknowledgements

We thank the Deutsche Forschungsgemeinschaft (SFB 807 "Transport and Communication across Biological Membranes" and Cluster of Excellence "Macromolecular Complexes") for financial support. Ernst Winter is acknowledged for the construction of optomechanical devices and general technical support.

References

- [1] O. Bèjà, L. Aravind, E.V. Koonin, M.T. Suzuki, A. Hadd, L.P. Nguyen, S. Jovanovich, C.M. Gates, R.A. Feldman, J.L. Spudich, E.N. Spudich, E.F. DeLong, *Science* 289 (2000) 1902–1906.
- [2] O. Bèjà, E.N. Spudich, J.L. Spudich, M. Leclerc, E.F. DeLong, *Nature* 411 (2001) 786–789.
- [3] D.L. Man, W.W. Wang, G. Sabehi, L. Aravind, A.F. Post, R. Massana, E.N. Spudich, J.L. Spudich, O. Bèjà, *EMBO J.* 22 (2003) 1725–1731.
- [4] D. Man-Aharonovich, G. Sabehi, O.A. Sineshchekov, E.N. Spudich, J.L. Spudich, O. Bèjà, *Photochem. Photobiol. Sci.* 3 (2004) 459–462.
- [5] G. Sabehi, R. Massana, J.P. Bielawski, M. Rosenberg, E.F. DeLong, O. Bèjà, *Environ. Microbiol.* 5 (2003) 842–849.

- [6] W.W. Wang, O.A. Sineshchekov, E.N. Spudich, J.L. Spudich, *J. Biol. Chem.* 278 (2003) 33985–33991.
- [7] A.K. Sharma, J.L. Spudich, W.F. Doolittle, *Trends Microbiol.* 14 (2006) 463–469.
- [8] A.L. Klyszejko, S. Shastri, S.A. Mari, H. Grubmüller, D.J. Müller, C. Glaubitz, *J. Mol. Biol.* 376 (2008) 35–41.
- [9] S. Shastri, J. Vonck, N. Pfeleger, W. Haase, W. Kühlbrandt, C. Glaubitz, *Biochim. Biophys. Acta, Biomembr.* 1768 (2007) 3012–3019.
- [10] L.C. Shi, M.A.M. Ahmed, W.R. Zhang, G. Whited, L.S. Brown, V. Ladizhansky, *J. Mol. Biol.* 386 (2009) 1078–1093.
- [11] J. Yang, L. Aslimovska, C. Glaubitz, *J. Am. Chem. Soc.* 133 (2011) 4874–4881.
- [12] J.J. Amsden, J.M. Kralj, L.R. Chieffo, X.H. Wang, S. Erramilli, E.N. Spudich, J.L. Spudich, L.D. Ziegler, K.J. Rothschild, *J. Phys. Chem. B* 111 (2007) 11824–11831.
- [13] A.K. Dioumaev, J.M. Wang, Z. Balint, G. Váró, J.K. Lanyi, *Biochemistry* 42 (2003) 6582–6587.
- [14] T. Friedrich, S. Geibel, R. Kalmbach, I. Chizhov, K. Ataka, J. Heberle, M. Engelhard, E. Bamberg, *J. Mol. Biol.* 321 (2002) 821–838.
- [15] Y. Furutani, D. Ikeda, M. Shibata, H. Kandori, *Chem. Phys.* 324 (2006) 705–708.
- [16] D. Ikeda, Y. Furutani, H. Kandori, *Biochemistry* 46 (2007) 5365–5373.
- [17] R.A. Krebs, D. Dunmire, R. Partha, M.S. Braiman, *J. Phys. Chem. B* 107 (2003) 7877–7883.
- [18] N. Pfeleger, M. Lorch, A.C. Wörner, S. Shastri, C. Glaubitz, *J. Biomol. NMR* 40 (2008) 15–21.
- [19] Y.W. Xiao, R. Partha, R. Krebs, M. Braiman, *J. Phys. Chem. B* 109 (2005) 634–641.
- [20] R. Rangarajan, J.F. Galan, G. Whited, R.R. Birge, *Biochemistry* 46 (2007) 12679–12686.
- [21] J.R. Hillebrecht, J. Galan, R. Rangarajan, L. Ramos, K. McCleary, D.E. Ward, J.A. Stuart, R.R. Birge, *Biochemistry* 45 (2006) 1579–1590.
- [22] A.K. Dioumaev, L.S. Brown, J. Shih, E.N. Spudich, J.L. Spudich, J.K. Lanyi, *Biochemistry* 41 (2002) 5348–5358.
- [23] H. Luecke, B. Schobert, J. Stagno, E.S. Imasheva, J.M. Wang, S.P. Balashov, J.K. Lanyi, *Proc. Natl. Acad. Sci. USA* 105 (2008) 16561–16565.
- [24] F. Hempelmann, S. Höpfer, M.-K. Verhoeven, A. Wörner, T. Köhler, S.-A. Fiedler, N. Pfeleger, J. Wachtveitl, C. Glaubitz, *J. Am. Chem. Soc.* 133 (2011) 4645–4654.
- [25] N. Pfeleger, A.C. Wörner, J. Yang, S. Shastri, U.A. Hellmich, L. Aslimovska, M.S.M. Maier, C. Glaubitz, *Biochim. Biophys. Acta, Bioenerg.* 1787 (2009) 697–705.
- [26] V.B. Bergo, O.A. Sineshchekov, J.M. Kralj, R. Partha, E.N. Spudich, K.J. Rothschild, J.L. Spudich, *J. Biol. Chem.* 284 (2009) 2836–2843.
- [27] É. Lörinczi, M.-K. Verhoeven, J. Wachtveitl, A.C. Wörner, C. Glaubitz, M. Engelhard, E. Bamberg, T. Friedrich, *J. Mol. Biol.* 393 (2009) 320–341.
- [28] G. Váró, L.S. Brown, M. Lakatos, J.K. Lanyi, *Biophys. J.* 84 (2003) 1202–1207.
- [29] M.O. Lenz, R. Huber, B. Schmidt, P. Gilch, R. Kalmbach, M. Engelhard, J. Wachtveitl, *Biophys. J.* 91 (2006) 255–262.
- [30] M. Lakatos, J.K. Lanyi, J. Szakacs, G. Váró, *Biophys. J.* 84 (2003) 3252–3256.
- [31] K. Neumann, M.-K. Verhoeven, I. Weber, C. Glaubitz, J. Wachtveitl, *Biophys. J.* 94 (2008) 4796–4807.
- [32] C.D. Heyes, M.A. El-Sayed, *J. Biol. Chem.* 277 (2002) 29437–29443.
- [33] G. Váró, J.K. Lanyi, *Biophys. J.* 59 (1991) 313–322.
- [34] G. Schäfer, S. Shastri, M.-K. Verhoeven, V. Vogel, C. Glaubitz, J. Wachtveitl, W. Mantele, *Photochem. Photobiol.* 85 (2009) 529–534.
- [35] A. Rupenyan, I.H.M. van Stokkum, J.C. Arents, R. van Grondelle, K. Hellingerwerf, M.L. Groot, *Biophys. J.* 94 (2008) 4020–4030.
- [36] V. Bergo, J.J. Amsden, E.N. Spudich, J.L. Spudich, K.J. Rothschild, *Biochemistry* 43 (2004) 9075–9083.
- [37] B. Aton, R.H. Callender, B. Becher, T.G. Ebrey, *Biochemistry* 16 (1977) 2995–2999.
- [38] R. van den Berg, D.J. Jang, H.C. Bittling, M.A. El-Sayed, *Biophys. J.* 58 (1990) 135–141.
- [39] M.S. Braiman, T. Mogi, T. Marti, L.J. Stern, H.G. Khorana, K.J. Rothschild, *Biochemistry* 27 (1988) 8516–8520.
- [40] K. Gerwert, B. Hess, J. Soppa, D. Oesterhelt, *Proc. Natl. Acad. Sci. USA* 86 (1989) 4943–4947.
- [41] W. Doster, *Biochim. Biophys. Acta, Proteins Proteomics* 1804 (2010) 3–14.
- [42] C. Gergely, L. Zimányi, G. Váró, *J. Phys. Chem. B* 101 (1997) 9390–9395.
- [43] E.S. Imasheva, K. Shimono, S.P. Balashov, J.M. Wang, U. Zadok, M. Sheves, N. Kamo, J.K. Lanyi, *Biochemistry* 44 (2005) 10828–10838.
- [44] E.S. Imasheva, S.P. Balashov, J.M. Wang, A.K. Dioumaev, J.K. Lanyi, *Biochemistry* 43 (2004) 1648–1655.
- [45] A.K. Dioumaev, L.S. Brown, R. Needleman, J.K. Lanyi, *Biochemistry* 38 (1999) 10070–10078.
- [46] C. Zscherp, J. Heberle, *J. Phys. Chem. B* 101 (1997) 10542–10547.
- [47] C. Zscherp, R. Schlesinger, J. Heberle, *Biochem. Biophys. Res. Commun.* 283 (2001) 57–63.
- [48] Y. Cao, G. Váró, A.L. Klinger, D.M. Czajkowsky, M.S. Braiman, R. Needleman, J.K. Lanyi, *Biochemistry* 32 (1993) 1981–1990.
- [49] S. Szaraz, D. Oesterhelt, P. Ormos, *Biophys. J.* 67 (1994) 1706–1712.
- [50] F. Garczarek, K. Gerwert, *Nature* 439 (2006) 109–112.
- [51] B. Hessling, G. Souvignier, K. Gerwert, *Biophys. J.* 65 (1993) 1929–1941.
- [52] H. Kandori, Y. Yamazaki, J. Sasaki, R. Needleman, J.K. Lanyi, A. Maeda, *J. Am. Chem. Soc.* 117 (1995) 2118–2119.
- [53] R. Rammelsberg, G. Huhn, M. Lübken, K. Gerwert, *Biochemistry* 37 (1998) 5001–5009.
- [54] C. Zscherp, R. Schlesinger, J. Tittor, D. Oesterhelt, J. Heberle, *Proc. Natl. Acad. Sci. USA* 96 (1999) 5498–5503.
- [55] J. Heberle, J. Fitter, H.J. Sass, G. Büldt, *Biophys. Chem.* 85 (2000) 229–248.
- [56] S. Wolf, E. Freier, K. Gerwert, *ChemPhysChem* 9 (2008) 2772–2778.
- [57] S. Wolf, E. Freier, M. Potschies, E. Hofmann, K. Gerwert, *Angew. Chem. Int. Ed Engl.* 49 (2010) 6889–6893.